Development of a Filtering Respirator with a Real-Time Monitoring Device for Pressure Drop

Розробка фільтрувального респіратора з пристроєм оперативного контролю перепаду тиску

Yurii Cheberiachko
Corresponding author: Dr of Technical Sciences, Professor, Department of Labor Protection and Civil Security, e-mail: cheberiachko.yu.i@nmu.one, ORCID ID: https://orcid.org/0000-0001-7307-1553

Dmytro Radchuk
Candidate of Technical Sciences, Associate Professor, Department of Labor Protection and Civil Security, e-mail: xayal1333@gmail.com, ORCID ID: https://orcid.org/0000-0001-8034-541X

Serhii Cheberiachko
Dr of Technical Sciences, Professor, Department of Occupational Safety and Civil Security, e-mail: xayal1333@gmail.com, ORCID ID: https://orcid.org/0000-0003-3281-7157

Dmytro Slavinskyi
Candidate of Technical Sciences, Associate Professor, Department of Cyber-Physical and Information-Measuring Systems, e-mail: xayal1333@gmail.com, ORCID ID: https://orcid.org/0000-0002-7540-2077

Bohdan Kravchenko
Assistant, Department of Labor Protection and Civil Security, e-mail: xayal1333@gmail.com, ORCID ID: https://orcid.org/0000-0001-8398-0793

Dnipro University of Technology, Dnipro, Ukraine

Юрій Чеберячко
Corresponding author: доктор технічних наук, професор, кафедра охорони праці та цивільної безпеки, e-mail: cheberiachko.yu.i@nmu.one, ORCID ID: https://orcid.org/0000-0001-7307-1553

Дмитро Радчук
кандидат технічних наук, доцент, кафедра охорони праці та цивільної безпеки, e-mail: xayal1333@gmail.com, ORCID ID: https://orcid.org/0000-0001-8034-541X

Сергій Чеберячко
доктор технічних наук, професор, кафедра охорони праці та цивільної безпеки, e-mail: xayal1333@gmail.com, ORCID ID: https://orcid.org/0000-0003-3281-7157

Дмитро Славінський
кандидат технічних наук, доцент, кафедра кіберфізичних та інформаційно-вимірювальних систем, e-mail: xayal1333@gmail.com, ORCID ID: https://orcid.org/0000-0002-7540-2077

Богдан Кравченко
Асистент, кафедра охорони праці та цивільної безпеки, e-mail: xayal1333@gmail.com, ORCID ID: https://orcid.org/0000-0001-8398-0793

Національний технічний університет "Дніпровська політехніка", м. Дніпро, Україна

Received: January 22, 2026 | Revised: February 19, 2026 | Accepted: February 28, 2026

UDC 614.894:331.45

DOI: https://doi.org/10.33445/sds.2026.16.1.16

Purpose. Development of a filtering respirator with a device for operational pressure drop control.

Method: The development of the filtering respirator with a real-time pressure drop monitoring device involved the use of the following equipment: the ESP32-C6-LCD-1.47 microcontroller with a video display, and the MPXV7002DP FRS pressure sensor, which enable monitoring of the pressure drop caused by dust accumulation, based on determining the critical filter resistance value.

Findings. A real-time monitoring device for pressure drop in the respirator filter cartridge has been developed. It provides contributes to improved worker safety in hazardous conditions and extends the possibilities of personalizing respiratory protective equipment according to specific operational requirements and users' physiological characteristics. The developed algorithm of the device enhanced the protective properties of the filtering respirator by timely informing the user about the pressure drop status of the filter, which is associated with half-mask tightness and battery charge level. A mathematical model has been proposed, correlating filter parameters, breathing mode, and the characteristics of the pressure drop sensor, which allows for determining changes in the pressure drop across the filter element depending on dust accumulation on the filter surface. This makes it possible to control filter service life by comparing it with the critical pressure drop value.

Paper type. Experimental studies of filtering respirator' performance indicators.

Мета дослідження. Розробка фільтрувального респіратора з пристроєм оперативного контролю перепаду тиску.

Метод дослідження. Розробка фільтрувального респіратора з пристроєм оперативного контролю перепаду тиску передбачає використання наступного обладнання: мікроконтролер ESP32-C6-LCD-1.47 з відео дисплеєм та датчик для контролю тиску MPXV7002DP FRS, які дозволяють забезпечити контроль перепаду тиску при накопиченні пилового осаду на основі визначення критичної величину опору фільтрів.

Результати дослідження. Розроблено пристрій оперативного контролю перепаду тиску на фільтрувальній коробці респіратора, який створює передумови для підвищення рівня безпеки працівників у шкідливих умовах праці та розширює можливості персоналізації засобів індивідуального захисту відповідно до специфічних операційних вимог та фізіологічних особливостей користувачів. Розроблений алгоритм роботи пристрою оперативного контролю перепаду тиску на фільтрувальній коробці респіратора підвищує захисні властивості фільтрувального респіратору завдяки своєчасному інформуванню користувача про стан перепаду тиску фільтру, що взаємопов'язано з герметичністю півмаски та рівнем заряду батареї. Запропоновано математичну модель, яка взаємопов'язує параметри фільтра, режим дихання і характеристики датчика перепаду тиску, що дозволяє визначати зміну перепаду тиску на фільтруючому елементі у залежності від накопичення пилового осаду на поверхні фільтра задля контролю часу експлуатації фільтрів шляхом порівняння з критичною величиною перепаду тиску.

Тип статті. Експериментальні дослідження показників фільтрувальних респіраторів.

Key words: Filtering Respirator, Pressure Drop, Mathematical Model, Real-Time Monitoring Device for Pressure Drop, Protective Efficiency of Respirator.

Ключові слова: фільтрувальний респіратор, перепад тиску, математична модель, пристрій оперативного контролю перепаду тиску, захисна ефективність респіратора.

Introduction

The pressure drop across respirator filters is one of the key parameters that influences the protective efficiency of the filter and determines the safe service life of the respirator (Cheberyachko, 2013). When the critical pressure drop threshold is reached, the protective efficiency of the respirator may deteriorate due to significant suction of unfiltered air through gaps between the user's face and the half-mask respirator (Roberge, 2011). On the other hand, a dust-loaded filter causes breathing difficulties. Currently, each user independently decides when to replace the filter, based on the onset of discomfort caused by increased breathing resistance (Srijit, 2020). This subjective factor complicates the calculation of the required number of filters when respirators are used under dusty air conditions. Therefore, to standardize filter replacement intervals, it is essential to address the urgent task of ensuring real-time monitoring of pressure drop across filters.

Literature review

In (Shin, 2022), the authors proposed a system for measuring the user's breathing rate using an air pressure sensor in the respirator. They noted that such sensors are inexpensive and energy-efficient, resulting in only a minor increase in respirator cost. At the same time, the economic effect of reducing inefficient filter usage makes this improvement attractive.

In (Pei, 2023), the authors developed an intelligent filter performance monitoring system capable of measuring filtration efficiency, pressure drop, temperature, and relative humidity in real time. This not only makes it possible to determine the protective service life of filters but also enables monitoring of workers' dust exposure levels, thereby helping to prevent occupational diseases.

Based on their research (2023), the authors developed a "smart" N-95 respirator that combines a humidity sensor and a pressure sensor to adaptively adjust half-mask fit to the face in order to maintain protective efficiency. In the event of mask slippage or air leakage through gaps, a signal is generated to indicate deterioration of protective properties, requiring corrective user action.

In (Aqueveque, 2022), an embedded electronic device is described that collects multidimensional data from an integrated pressure, temperature, and relative humidity sensor inside a reusable industrial respirator. The device calculates breathing rate and evaluates both respirator fit to the face and pressure drop during dust accumulation.

The authors of (Roberge, 2013) emphasize the importance of solving the task of pressure drop monitoring. They provide arguments demonstrating the feasibility of implementing intelligent pressure drop monitoring systems in respirator use.

The study (Cao, 2015) highlights the role of differential pressure sensors in testing protective masks to evaluate filter resistance and efficiency under production conditions, which differ from laboratory ones and do not allow for reliable determination of protective service periods.

The analysis of scientific studies confirms the relevance of ensuring pressure drop monitoring, which enables the solution of several tasks—from controlling filter dust loading and calculating the required number of filters per work shift to determining the service life of the filter.

Aim of the work – development of a filtering respirator with a real-time pressure drop monitoring device.

Materials and Methods

The development of the filtering respirator with a real-time pressure drop monitoring device involved the use of the following equipment: a microcontroller with video display and a pressure sensor.

The microcontroller is based on the modular printed circuit board ESP32-C6-LCD-1.47 (Fig. 1) based on ESP32, which is based on the Tensilica Xtensa microprocessor. In addition, the ESP32-C and -S series boards use a 32-bit Risc-V processor model (single- and dual-core variants) instead of Xtensa. The RISC-V architecture is open-source and facilitates flexible system integration. In addition, these boards allow combined Wi-Fi and Bluetooth connectivity (supports Wi-Fi 6 in the 2,4 GHz band, Bluetooth 5, Zigbee 3.0 and Thread 1.3); support all standard IEEE 802.11 security features, including WFA, WPA/WPA2 and WAPI, and have open-source software and open SDK (Software Development Kit – a set of tools, libraries, documentation and code samples). The ESP32-C6-LCD-1.47 development board has an integrated matrix TFT LCD module LBS147TC-IF15 measuring 17,4x32,4 mm, with a resolution of 172x320 pixels and 262 thousand colors.

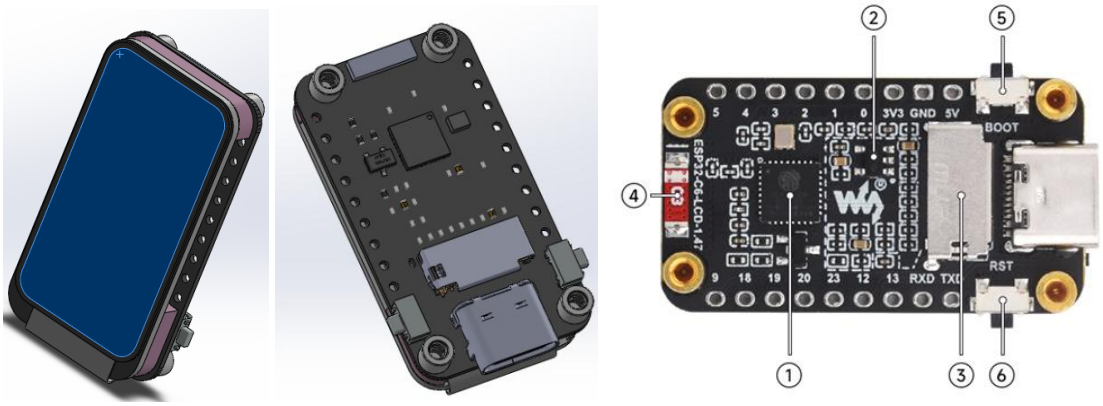

Figure 1: ESP32-C6-LCD-1.47 Development Board
1) ESP32-C6FH4 microchip; 2) ME6217C33M5G voltage regulator; 3) TF (SD) card slot;
4) Surface-mount ceramic antenna; 5) LOAD button; 6) RESET button

To determine the resistance of the filtering element(s) or the pressure drop on the respirator filter housing, a differential pressure sensor MPXV7002DP FRS (±2 kPa) was used, which has an analog output signal U_{out} = ±2,5 V (Fig. 2).

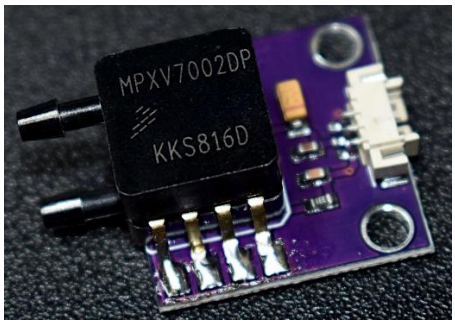

Figure 2: Appearance of the MPXV7002DP FRS Pressure Sensor

According to the technical documentation, the system components have the following current consumption: ESP32-C6 chip at 25 mA (at 80 MHz); matrix TFT LCD module 15 mA; differential pressure sensor up to 10 mA. Thus, the total current is 50 mA. Considering the 3,3 V supply, the power consumption of the system will be 3,3 · 0,05 = 0,165 W.

The required rechargeable battery capacity (Bazaluk, 2021) was calculated using the formula:

$$C = \frac{P \cdot t}{U}, \quad (1)$$

where C – battery capacity (Ah);
P – power consumption (W);
t – time (h);
U – battery voltage (V).

To ensure continuous operation of the device for 6 hours, the capacity of the accumulator with a voltage of 3,7 V will be: $0{,}268\ \text{A} \cdot \text{h}$. Considering the standard nominal range of rechargeable batteries and taking into account the necessary capacity reserve of 20 %, we can accept for use an accumulator with a voltage of 3,7 V and a capacity of 320 mA·h, Li-Ion GEB10440 320mAh, 3,7V.

One of the key aspects that affects the efficiency of the filter operation is the gradual increase in its resistance due to dust accumulation on the surface, so for calibrating the pressure sensor, the formula that relates the increase in pressure drop due to dust accumulation (Cheberiachko, 2023) was used:

$$\Delta p_{заг} = \Delta p_o + \frac{k_n \rho_n \phi F_0^2}{3\pi^2 L}\left[\left(F_B^2 + \frac{\Pi_\phi F_B}{a \rho_n \phi F_0}\right)^{3/2} - F_B^3\right], \quad (2)$$

where Δp_o – is the initial resistance of a clean filter, Pa;
k_n – is the proportionality coefficient depending on the filtration rate, m⁴/s²;
ρ_n – is the bulk density of dust particles, kg/m³;
φ – is the coefficient of non-uniformity of dust distribution on filter fibers;
F_B – is the total surface area of the filter fibers;
L – is the total length of fibers in the filter, m⁻¹;
Π_f – is the mass of accumulated dust on the filter, mg.

The dust mass is calculated using the formula (Diekman, 2017):

$$\Pi_f = \frac{2CQt}{F_0}, \quad (3)$$

where C – is the total dust concentration, mg/m³;
Q – is the volumetric air flow through the filter, m³/s;
t – is the respirator operating time interval, s;
F_o – is the total filter area, m².

The total length of fibers and their total area were determined using the formulas (Bergman, 2017):

$$L = \frac{\beta \cdot H}{\pi \cdot a^2}, \quad (4)$$

$$F_B = \frac{2bH}{a}, \quad (5)$$

where β – is the fiber packing density;
H – is the thickness of the filter layer, m; a is the average radius of fibers in the filter, m.

Based on formula (2), a block diagram is constructed for modeling real-time pressure drop monitoring on the respirator (Fig. 3), taking into account the breathing process, operating time monitoring, determination of dust concentration in the working area, and air flow through the filter. The overall algorithm of the real-time pressure drop monitoring system on the respirator is shown in Fig. 4.

After switching on the toggle switch that supplies power to the control and information processing unit, the system initializes the processor core and peripheral devices. A file is created on

the memory card to store data on respirator operation. This process includes configuring the SPI bus to enable interaction between the microcontroller and the memory card. Input/output ports are identified to verify the system's readiness for operation. This function ensures that all components are prepared for subsequent operations, providing a foundation for uninterrupted collection and storage of data on respirator performance throughout the work shift.

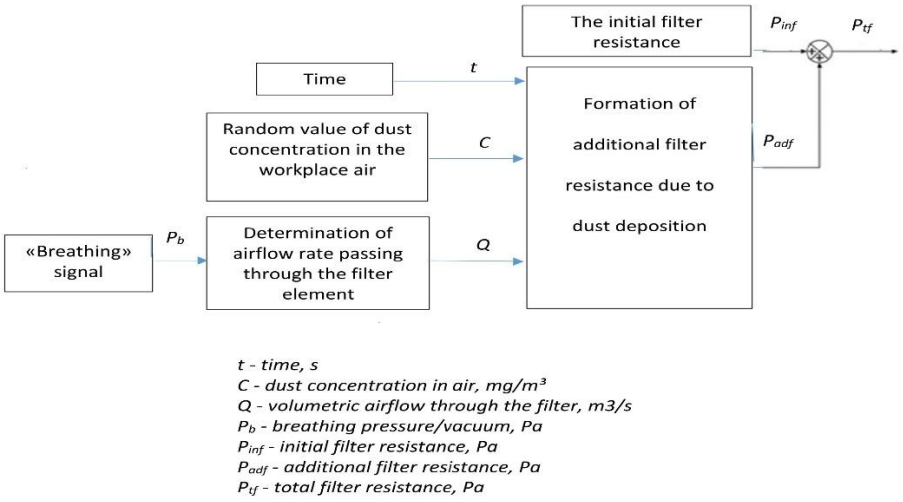

Figure 3: Structural diagram of the mathematical model of the respirator for determining the dependence of the pressure drop change on the filtering element depending on dust accumulation

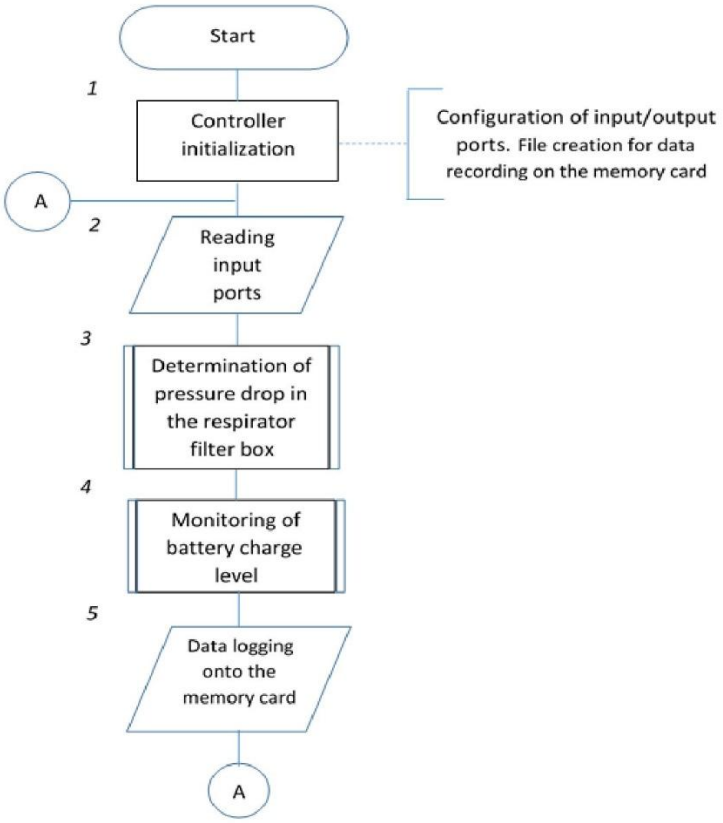

Figure 4: General algorithm of the pressure drop control system operation on the respirator

Real-time pressure drop monitoring on the respirator filter housing is carried out by comparing the measured pressure drop during breathing with stored critical values that indicate the need for filter replacement.

The signal from the sensor, which has a voltage range of 0-5 V, was converted by a 10-bit analog-to-digital converter into integer values from 0 to 1023. Over time, as dust accumulates on the filter, breathing resistance increases, which is detected by the pressure sensor. When the pressure drop reaches the first critical level (70 Pa at an airflow of 30 L/min; for other airflow rates, it is calculated using a laboratory-determined dependence, Fig. 5), indicating partial contamination, the control unit activates a warning signal. If operation continues, the dust mass on the filter increases, reaching the second critical pressure drop level (100 Pa at 30 L/min), at which the respirator's protective efficiency may decrease. The control system will activate a red LED and emit short audible signals, notifying the user that the filter housing needs to be replaced.

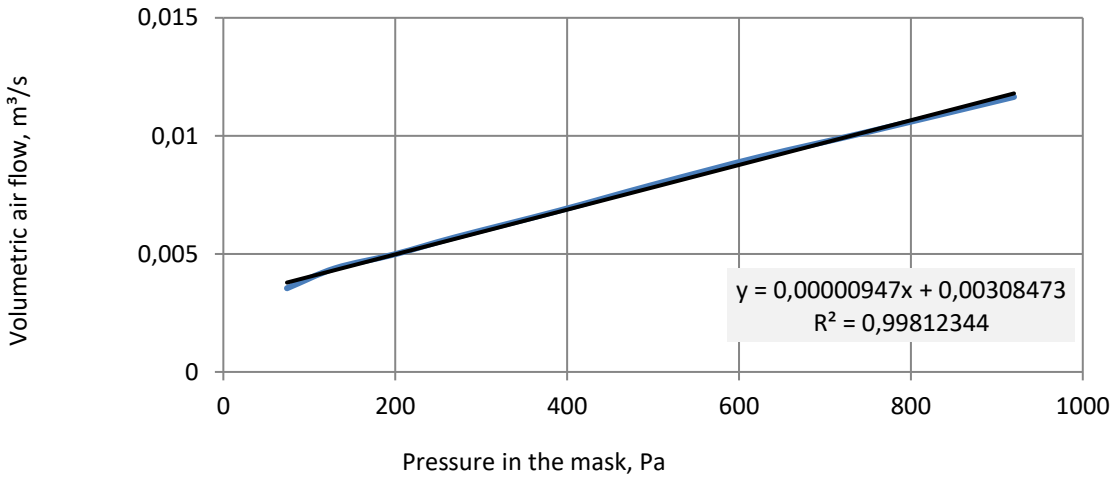

Figure 5: Dependence of the pressure drop on filters on the volumetric air flow for determining the critical pressure drop value

A decrease in protective efficiency occurs due to significant breathing resistance (established for each type of respirator under laboratory conditions), which leads to the appearance of air leaks through gaps in the respirator sealing strip. This moment is detected by the sensor as a certain drop in pressure after a continuous increase, indicating the emergence of additional airflow paths into the under-mask space.

Battery level monitoring, which powers the control system and the pressure sensor, is performed using a voltage divider connected to the microcontroller's analog port. The system reads the voltage, which is proportional to the charge level, and compares it with preset threshold values. The battery level indicator displays the current status of the power source. If the charge drops to a critical level, the system issues a corresponding signal, notifying the user of the need to replace or recharge the battery. This function ensures uninterrupted device operation and prevents unexpected shutdown due to battery depletion.

After each pressure sensor polling cycle, the system records data on pressure, filter condition, and battery level onto the memory card. This process occurs via the SPI bus, which provides fast and reliable data exchange. The stored information includes respirator operation parameters throughout the work shift. Through a data extraction port, the information can be transferred to an external device for further processing, for example, to analyze respirator usage efficiency or verify compliance with safety requirements. This function enables operational tracking of the device, which is important for monitoring its condition and evaluating operating conditions.

Each of the described functions operates within a general cycle, which repeats to ensure continuous monitoring of respirator parameters. Together, these components form a reliable system that enhances the protective performance of the device and improves user convenience. The system optimizes operational characteristics by providing timely information on filter condition, half-mask seal integrity, and battery charge level. A general view of the respirator filter housing with the real-time pressure drop monitoring device is shown in Fig. 6.

Figure 6: General view of the real-time pressure drop monitoring unit on respirator filters with display

Results

At the first stage, the operation of the real-time pressure drop monitoring unit during breathing was evaluated under different operating modes, with airflow rates ranging from 30 to 95 L/min. The obtained values were compared with available experimental data published to verify the performance of the pressure drop sensor. Approximation of the experimental and theoretical data using the normalized root mean square error "NRMSE", calculated in MATLAB with the "goodnessOfFit" function (Stafford, 1973), was 88,74%, with a correlation coefficient of 0,94 and Fisher's statistical criterion of 10256. The dependence of the filter element resistance on varying airflow rates from 30 to 95 L/min is shown in Fig. 7.

The next stage involved testing the operation of the pressure drop monitoring unit during breathing under different user operating modes with dusty filters. The dust concentration was 300 mg/m³. The filtration surface area of a single filter element was 0,00785 m² (filter cartridge diameter 100 mm). The initial filter resistance was 27 Pa at 30 L/min. The filter was made of Eleflen material with an average fiber diameter of 2,5 µm. The fiber packing surface density was 55 mg/m², and the proportionality coefficient dependent on filtration velocity was 1,4 m⁴/s². The bulk density of dust particles was 1,6 kg/m³, and the non-uniformity coefficient of dust distribution on the fibers was 1.2.

Experimental pressure data for similarly dust-loaded filters, used for comparison, were published in studies (Yao, 2019; Qiang, 2022). The results are shown in Fig. 8. The data approximation of experimental and theoretical data by the normalized root mean square error "NRMSE", calculated in MATLAB using the "goodnessOfFit" function (Stafford, 1973), is 58,74 %, the correlation coefficient was 0.915, Fisher's statistical criterion is 10273. This indicates sufficient reliability of the mathematical model, which allows its use in further studies of the operational pressure drop control unit.

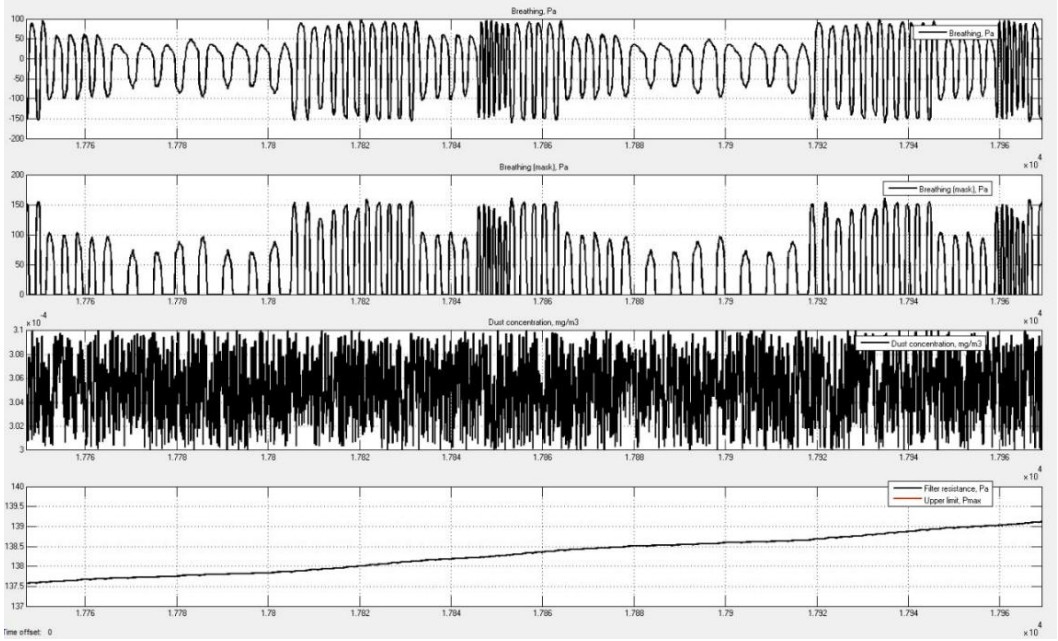

Figure 7: Dependence of filter element resistance on changes in air flow ranging from 30 to 95 L/min

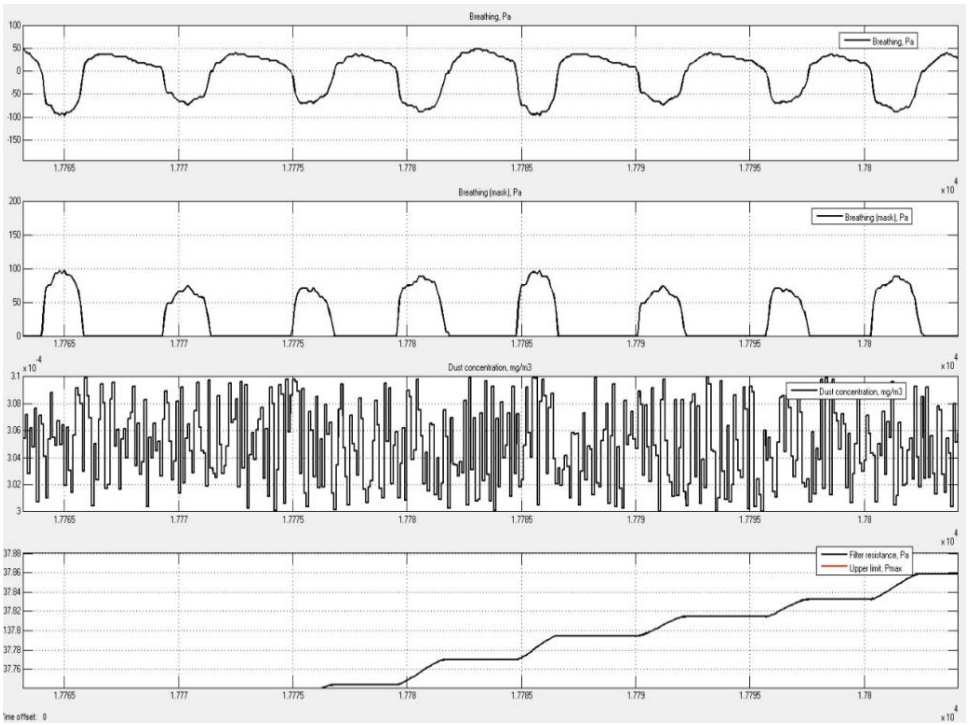

Figure 8: Change in Pressure Drop on the Filtering Element at Dustiness of 300 mg/m³

Discussion

The main technical outcome is the determination of the required number of filters to protect the user under high dust conditions, taking into account the operating mode, based on an algorithm for calculating filter replacement time. This algorithm is based on real-time monitoring of pressure drop changes due to dust accumulation on the filter surface. This is achieved through:

determining the critical level of filter contamination through the change in the mechanical position of the lever system associated with the movable partition;

processing pressure data using a linear regression algorithm taking into account breathing cycles, which increases the accuracy of the forecast;

displaying information about the residual resource of the reusable replaceable filter cartridge with a filter for respirators on the display and saving it for analysis;

optimizing costs through timely replacement of filters and pre-filters, as well as planning the required quantity.

The proposed technology provides indirect control of dust mass on the filter through mechano-electrical interaction, which allows accurately determining the filter replacement time in the filter cartridge for respirators without the need for direct weighing.

The calculation results are displayed on the screen in the form of the time remaining until filter replacement and are stored in the device's memory. The user receives understandable data for work planning, and organizations – statistics for calculating the required number of filters. This approach may reduce operational costs associated with premature filter replacement; however, quantitative cost analysis is required. Automated control eliminates the human factor, and forecasting based on data ensures system reliability. The proposed approach may be particularly applicable in mining, metallurgical, and construction industries characterized by high dust concentrations.

Conclusion

A real-time pressure drop monitoring device for the respirator filter housing was developed, providing the basis for enhanced worker safety in hazardous working conditions and expanding possibilities for personalizing protective equipment according to specific operational requirements and user physiological characteristics.

The developed real-time pressure drop monitoring algorithm improves the protective properties of the filtering respirator by timely informing the user about the filter's pressure drop status, which is correlated with half-mask seal integrity and battery charge level.

A mathematical model was proposed linking filter parameters, breathing mode, and pressure sensor characteristics, enabling determination of pressure drop changes on the filter element depending on dust accumulation, thereby controlling filter service life by comparison with the critical pressure drop value.

Acknowledgments

Holinko V. I., Head of the Department of Occupational Safety and Civil Protection, Dnipro University of Technology; M.S. Vasylchenko, Director of the company "NVP Standart".

Funding

This study received no specific financial support.

Competing interests

The authors declare that they have no competing interests.

References

1. Cheberyachko, S.I., Yavors'ka, O.O., Morozova, T.I. (2013). Study of mechanical half-mask pressure along obturation bar. *Mining of Mineral Deposits*, pp. 317-323.
2. Roberge, R.J., Monaghan, W.D., Palmiero, A.J. et al. (2011). Infrared imaging for leak detection of N95 filtering facepiece respirators: A pilot study. *American Journal of Industrial Medicine*, Vol. 54, pp. 628-636.
3. Srijit, D., Sakthiswary, R. (2020). Personal protective equipment (PPE) and its use in COVID-19: important facts. *Indian Journal of Surgery*, pp. 1-2. DOI: https://doi.org/10.1007/s12262-

020-02411-8.
4. Shin, W. (2022). A Study on the Measurement of Respiratory Rate Using a Respirator Equipped with an Air Pressure Sensor. International Journal of Advanced Smart Convergence, 11(4), pp. 240-246. DOI: https://doi.org/10.7236/IJASC.2022.11.4.240.
5. Pei, C., Chen, W., Ou, Q., Pui, D.Y.H. (2023). Smart Filter Performance Monitoring System. *Aerosol Air Qual, Res*. 23, 220416. DOI: https://doi.org/10.4209/aaqr.220416.
6. Novel Smart N95 Filtering Facepiece Respirator with Real-time Adaptive Fit Functionality and Wireless Humidity Monitoring for Enhanced Wearable Comfort // Kangkyu Kwon and Yoon Jae Lee and Yeong-Tae Jung and Ira Soltis and Chanyeong Choi and Yewon Na and Lissette Romero and Myung Chul Kim and Nathan Rodeheaver and Hodam Kim and Michael S. Lloyd and Ziqing Zhuang and William King and Susan Xu and Seung Hwan Ko and Jinwoo Lee and Woon-Hong Yeo. Journal ArXiv, 2023, 2309.07152, Available from: https://api.semanticscholar.org/CorpusID:261822598.
7. Aqueveque P, Díaz M, Gomez B, Osorio R, Pastene F, Radrigan L, Morales A. (2022). Embedded Electronic Sensor for Monitoring of Breathing Activity, Fitting and Filter Clogging in Reusable Industrial Respirators. Biosensors (Basel), Nov 8;12(11):991. DOI: https://doi.org/10.3390/bios12110991. PMID: 36354500; PMCID: PMC9688112.
8. Roberge, RJ., Kim, J-H., Powell, JB., Shaffer, RE., Ylitalo, CM., Sebastian, JM. (2013) Impact of Low Filter Resistances on Subjective and Physiological Responses to Filtering Facepiece Respirators. PLoS ONE 8(12): e84901. DOI: https://doi.org/10.1371/journal.pone.0084901.
9. Cao, Q., Pui, D.Y.H., Pui, D.Y.H., Lipiński, W. (2015). A concept of a novel solar-assisted large-scale cleaning system (Salscs) for urban air remediation. Aerosol Air Qual. Res. 15, pp. 1-10. DOI: https://doi.org/10.4209/aaqr.2014.10.0246.
10. Bazaluk, O., Ennan, A., Cheberiachko, S., Deryugin, O., Cheberiachko, Y., Saik, P., Lozynskyi, V., & Knysh, I. (2021). Research on Regularities of Cyclic Air Motion through a Respirator Filter. *Applied Sciences*, 11(7), 3157. DOI: https://doi.org/10.3390/app11073157.
11. Cheberiachko, S., Cheberiachko, Y., Deryugin, O., Kravchenko, B., Nehrii, T., Nehrii, S., & Zolotarova, O. (2023). Increasing the insulation properties of filter respirators to protect miners' respiratory organs from dust. Rudarsko-geološko-Naftni Zbornik, 38(4), pp. 27-40. DOI: https://doi.org/10.17794/rgn.2023.4.3.
12. Diekman, C.O., Thomas, P.J., & Wilson, C.G. (2017). Eupnea, tachypnea, and autoresuscitation in a closed-loop respiratory control model. *Journal of Neurophysiology*, 118, pp. 2194-2215. DOI: https://doi.org/10.1152/jn.00170.2017.
13. Bergman, M., Basu, R., Lei, Z., Niezgoda, G., & Zhuang, Z. (2017). Development of a Manikin-Based Performance Evaluation Method for Loose-Fitting Powered Air-Purifying Respirators. *Journal of The International Society for Respiratory Protection*, 34, pp. 40-57. Available from: https://pubmed.ncbi.nlm.nih.gov/30498287/
14. Stafford, R. G., Ettinger, H.J., & Rowland, T.J. (1973). Respirator Cartridge Filter Efficiency under Cyclic- and Steady-Flow Conditions. *American Industrial Hygiene Association Journal*, 34(5), pp. 182-192. DOI: https://doi.org/10.1080/0002889738506832.
15. Yao BG, Wang YX, Ye XY, Zhang F, Peng YL. (2019). Impact of structural features on dynamic breathing resistance of healthcare face mask. Sci Total Environ. Nov 1;689:743-753. DOI: https://doi.org/10.1016/j.scitotenv.2019.06.463. Epub 2019 Jun 28. PMID: 31280156.
16. Qiang Li, Zhichao Wang, Shuangquan Shao, Zhiqiang Niu, Yalu Xin, Dan Zhao, Yinyan Hou, Zhaowei Xu. (2022). Experimental study on the synthetic dust loading characteristics of air filters, Separation and Purification Technology, Volume 284, 120209, DOI: https://doi.org/10.1016/j.seppur.2021.120209.